22.2 A Rugged Wearable Modular ExG Platform Employing a Distributed Scalable Multi-Channel FM-ADC Achieving 101dB Input Dynamic Range and Motion-Artifact Resilience

Julian Warchall[1], Paul Theilmann[2], Yuxuan Ouyang[2], Harinath Garudadri[1], Patrick P. Mercier[1]

[1]University of California, San Diego, La Jolla, CA
[2]MaXentric Technologies, La Jolla, CA

Wearable ExG biopotential acquisition systems can potentially capture a wealth of clinically useful diagnostic information during activities of daily life. In practice, however, motions from common activities introduce large artifacts that can easily saturate traditional analog front-ends (AFEs) designed to sense biopotentials on the micro- to milli-volt scale. In addition, the wires that connect each electrode to an array of high-impedance AFEs can easily pick up interference and large, potentially saturating artifacts. For these reasons, many-channel monolithic biopotential sensing systems are often fragile and difficult to use in ambulatory environments. While active electrodes can be used to combat interference picked up by high-impedance wires, they require power-hungry drivers to deliver high-fidelity signals across relevant anatomy to an array of ADCs. Placing an ADC on each active electrode followed by a digital bus driver can eliminate analog driver power, resulting in a per-channel power consumption of 104μW in [1]. However, the 12b SAR ADC in [1] could not tolerate significant motion artifacts, and further increasing the ADC resolution to accommodate a larger dynamic range (DR) would require a quadratic increase in per-channel ADC power consumption.

This paper presents a wearable *N*-channel FM-ExG platform, shown in Fig. 22.2.1, that achieves high-DR motion-artifact-resilient yet low-power operation in a modular and rugged form factor by: 1) coupling each ExG electrode to an active IC comprising a sinusoidal VCO, whose output is a bandwidth-expanded frequency-modulation (FM) signal, with FM coding gain cubically proportional to the bandwidth expansion factor; 2) aggregating multiple FM signals with frequency division multiplexing (FDM) over a single wire via energy-efficient tuned-amplifiers, where each FM-ExG signal rests at a distinct center frequency set by each VCO; 3) exploiting VCO-enabled FM coding gain to digitize all *N* channels simultaneously with a single 12b SAR ADC at a wearable gateway while achieving a per-channel SNR of 101dB; 4) operating the SAR ADC at the aggregate FM spectrum bandwidth (1.28MHz) rather than Nyquist (~30MHz) by exploiting the low-harmonic nature of the sinusoidal VCO and bandpass sampling, reducing ADC power from ~5.7mW to 190μW; and 5) transmitting the digitized FM spectrum via an energy-efficient UWB TX based on [2] for off-body processing and storage. While the distributed FM-ADC-like [3] nature of the system is similar to [4], this paper represents the first IC-based embodiment that fully realizes advantages in energy efficiency and system motion artifact reduction.

As depicted in Fig. 22.2.1, *N* active electrode ICs are daisy-chained via a 4-wire bus consisting of $V_{DD,}$ GND, an on-body reference potential, and the FDM wire. Each active electrode IC is attached to a skin-contact electrode via a coupling capacitor, and up-converts the ~250Hz BW biopotential voltage to a 50kHz BW FM-modulated signal. In practice, FM-modulated signals are sensitive to phase, and thus system SNR is limited either by the lower bound between FM coding gain and phase noise. To maintain >100dB SNR for the given FM coding gain, simulations in Fig. 22.2.2 (top right) reveal a phase noise requirement for the VCO of <-120dBc/Hz at a 10kHz offset. This requirement is achieved at low power by utilizing an external 0603 inductor with Q=50 in a folded cross-coupled 14MHz oscillator (Fig 2 bottom left). To reduce power by a factor of 2.7×, the oscillator utilizes the minimum size transistors necessary to maintain oscillation after larger start-up transistors are switched out. Since the VCO cannot directly drive the FDM wire, a bandpass amplifier tuned by another 0603 inductor and varactor followed by a source-follower for additional isolation is employed (Fig. 22.2.2 bottom right), for a net savings of 80× in power over a conventional wideband driver.

Figure 22.2.3 (top left) shows the spectrum of a single FM channel driven by a full-scale 10mV 10Hz sinusoidal test message, while Fig. 22.2.3 (top right) shows the signal after demodulation, where worst-case VCO V-to-F nonlinearities are shown. The demodulated SNR and SNDR for varying amplitudes are shown in Fig. 22.2.3 (bottom left), demonstrating a peak SNR of 101dB, a peak SNDR of 84dB, and a useable DR of 101dB. This design does not employ a gain amplifier prior to the VCO, and instead directly up-converts the electrode's baseband signal to the FM domain. This feature provides resilience to out-of-range artifacts or disturbances if sufficient guard band in the FM domain is available. To demonstrate this, a 100 mV DC step (ostensibly 10× the full-scale range of the VCO's input) is applied concurrent with a 10mV test sinusoid. The resulting demodulated output, shown in Fig. 22.2.3 (bottom right) with and without the input coupling capacitor, tracks the 10mV test sinusoid well throughout the disturbance.

To demonstrate multi-channel access, six active electrodes were daisy-chained and driven with six different 1mV test sinusoids at 10, 50, 90, 130, 170, and 210Hz; the spectrum of the FDM wire here is shown in Fig. 22.2.4 (top). After being received by the SAR ADC sampling at 1.28MS/s (thanks to bandpass sampling) and after demodulation, the six message signals are individually distinguishable without any cross-talk as shown in Fig. 22.2.4 (bottom). An arbitrary number of active electrodes can be daisy-chained to realize massively parallel ExG acquisition by increasing the ADC sampling frequency to accommodate the added FM bandwidth.

The short 4-wire bus used to chain active electrode ICs together and connect to the gateway IC affords a rugged structure unlike other ExG systems previously published other than [1]. To demonstrate the advantages offered, the FM-ExG system and an OpenBCI system were connected side-by-side to measure ECG on an ambulatory subject. Both systems recorded a differential waveform with six electrodes placed on the chest. As is clearly seen in transient and spectrum recordings from the V2 chest electrode in Fig. 22.2.5 (top), the FM-EXG system tolerated subject motion much better than the OpenBCI system – 2.9× better according to normalized cross-correlations between still and motion data. The FM-ExG system was also validated in a SSVEP EEG-based experiment; Figure 22.2.5 (bottom) shows the results acquired after the UWB output correctly indicating a 10Hz component that corresponds to the 10Hz screen flashing in the SSVEP experiment.

The active electrode ICs and gateway IC are both fabricated in a 65nm process. The active electrode ICs expend 212μW/channel, while the 12b SAR ADC in the gateway IC consumes 190μW at 1.28MS/s, both at 1.2V. The UWB TX, whose FCC-complying output spectrum is shown in Fig. 22.2.6 (top right), consumes 11pJ/pulse, and 8 pulses are transmitted per bit for a total energy cost of 88pJ/b. For 101dB SNR operation, each FM channel occupies 50kHz, and with 50kHz of guard band between channels, 12 total channels are supported in the developed FM-ExG system (with more channels capable simply by increasing the SAR sampling rate). The digitization of multiple channels via a single low-power SAR ADC cements the power advantage of the proposed system, where each channel achieves 101dB SNR, yet with an aggregate power consumption of only 228μW/channel without the UWB TX, and 340μW/channel with. Despite the increased bit rate per channel due to FM-based oversampling and the corresponding extra energy required from the UWB TX to transmit at a higher data rate, the power efficiency and DR of the system reflected in the Schreier FoM exceeds that of prior-art active electrode systems that include the power of electrode-to-gateway drivers, and also exceeds conventional AFE arrays that do not (Fig. 22.2.6, bottom). Note that in all cases the 88pJ/b energy from the UWB TX is assumed in order to normalize TX performance across references. A photograph of the FM-ExG active electrode board is shown in Fig. 22.2.6 (top left), while die photos are shown in Fig. 22.2.7.

Acknowledgements:
This work was supported in part by the U.S. Army Research Laboratory under Contract W911QX-16-C-0003, and in part by the National Science Foundation Graduate Research Fellowship under Grant DGE-1144086. The authors acknowledge W. David Hairston for help and advice.

References:
[1] J. Xu, et al., "24.7 A 60nV/√Hz 15-Channel Digital Active Electrode System for Portable Biopotential Signal Acquisition," *ISSCC Dig. Tech. Papers*, Feb. 2014.
[2] A. T. Phan, et al., "Energy-Efficient Low-Complexity CMOS Pulse Generator for Multiband UWB Impulse Radio," *IEEE TCAS-I*, vol. 55, no. 11, pp. 3552-3563, 2008.
[3] J. Warchall, et al., "A 678-μW Frequency-Modulation-Based ADC with 104-dB Dynamic Range in 44-kHz Bandwidth," *IEEE TCAS-II*,vol. 65, no. 10, pp. 1370-1374, 2018.
[4] J. Warchall, et al., "A Multi Channel EEG System Featuring Single-Wire Data Aggregation via FM-FDM Techniques," *IEEE ISCAS*, pp. 526-529, 2016.

 978-1-5386-8531-0/19/$31.00

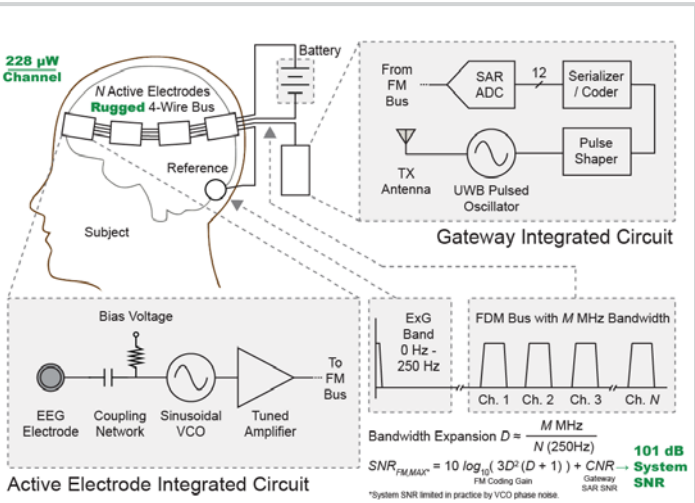

Figure 22.2.1: Top-level diagram of the FM-ExG system used for EEG with FM plan depicting N-channel frequency domain multiplexing.

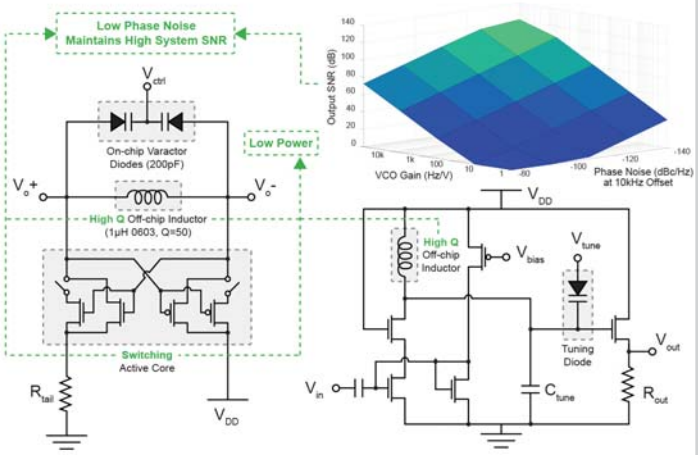

Figure 22.2.2: Circuit diagram of FM voltage-controlled oscillator (left); simulated effect of phase noise on an FM-FDM system's SNR (top right); circuit diagram of FM bus driving tuned bandpass amplifier (bottom right).

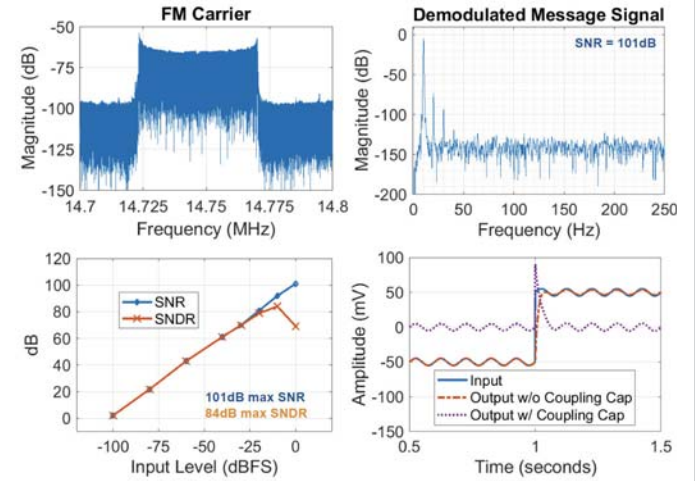

Figure 22.2.3: FFT of single channel driven with full-scale (10mV) 10Hz sine message (top left); same channel after demodulation (top right); system SNR and SNDR vs. input signal level (bottom left); demodulated transient step input interference for single channel configuration (bottom right).

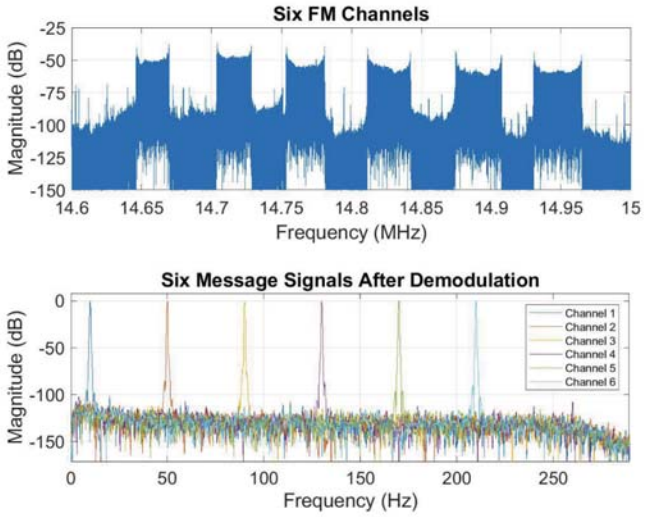

Figure 22.2.4: FFT of FDM bus for six channel test with various sine inputs (top); the six channels after demodulation, demonstrating spur-free DR (bottom).

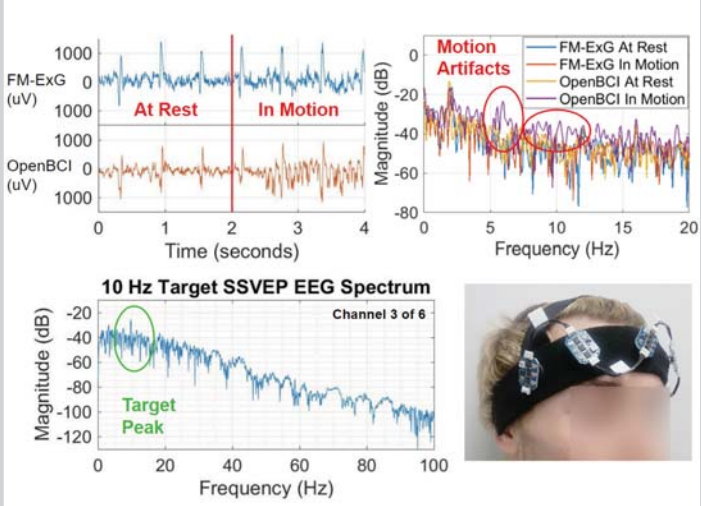

Figure 22.2.5: Demonstration of FM-ExG resilience to motion artifacts in ECG (top); FM-ExG system arranged for EEG application (bottom right); EEG spectrum from 10Hz SSVEP experiment using FM-ExG (bottom left).

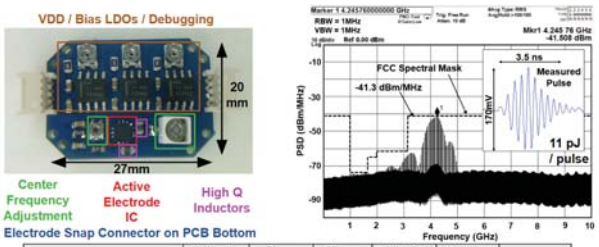

Design	Helleputte, JSSC 2015	Rieger, TCAS-I 2018	O'Leary, ISSCC 2018	Schöne, JSSC 2018	Xu, ISSCC 2014	This Work
Active Electrode?	No				Yes	
Process [nm]	180	180	130	130	180	65
IC Active Area [mm²]	49	0.06	7.6	20.8	15.8	1
Electrode Bus Drive Type	-	-	-	-	Digital I2C	FDM via Tuned Amplifier
Channels / Chip	5	3	32	9	1	1
IRN [uVrms] (BW)	0.61 (150Hz)	0.67 (100Hz)	1.6 (500Hz)	1.21 (150Hz)	0.65 (100Hz)	0.99 (250Hz) 0.63 (100Hz)
Acquisition Bandwidth [Hz]	250	7000	500	4000	100	250
Usable DR at Input [dB]	~83 (13.5-bit)	~50 (8-bit)	70	~83 (13.5-bit)	~74 (12-bit)	101
Output Bit Rate per Channel [Hz]	32000	56000	1000000	112000	2400	1280000
Acquisition Power per Channel [µW]	56	96.7	1.26	285	104.4	228
Calculated Wireless TX Power* per Channel [µW]	2.82	4.93	88	9.86	0.21	112.6
Total Power per Channel [µW]	58.82	101.63	89.26	294.86	104.61	340.6
FOM = Usable DR [dB] + 10 log10(BW [Hz] / Total Power per Channel [W])	149.3	128.4	137.5	154.3	133.8	159.7

*Calculated using 88 pJ/bit at digital output bit rate

Figure 22.2.6: Detail of active electrode application board (top left); Measured UWB pulse PSD showing FCC mask compliance (top right); Table of comparison (bottom).

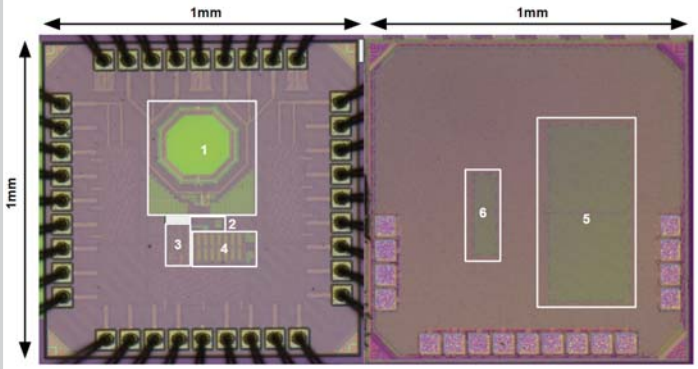

1 - UWB TX
2- Pulse Shaper
3 - Serializer/Coder
4 - SAR ADC
5 - Sinusoidal VCO
6 - Bandpass Tuned Amplifier

Figure 22.2.7: Die photo of gateway IC including SAR ADC and UWB TX (left); Die photo of active electrode IC including sinusoidal VCO and tuned amplifier (right).

978-1-5386-8531-0/19/$31.00